Green's function and lattice sums for electromagnetic scattering by a square array of cylinders

S.K. Chin and N.A. Nicorovici, and R.C. McPhedran
Department of Theoretical Physics, School of Physics, University of Sydney, New South Wales, Sydney, 2006, Australia
(Received 10 November 1993)

A method is given to represent in terms of absolutely convergent series the lattice sums involved in solving problems of electromagnetic diffraction by two-dimensional periodic arrays of obstacles. The expressions of the lattice sums are used to express the Green's function of the problem as a Neumann series. These results lead to very efficient algorithms for numerical calculations of the Green's function.

PACS number(s): 03.50.De, 41.20.Jb

I. INTRODUCTION

In general, the solution of the problem of electromagnetic diffraction by periodic arranged obstacles, using Rayleigh's method [1], involves a set of lattice sums. These quantities consist of sums over terms with a function evaluated at each lattice point. Depending on the kind of periodicity, different lattice sums associated with different functions may emerge.

The evaluation of lattice sums is the most difficult part of the whole of Rayleigh's method. The main reason is that the lattice sums are only conditionally convergent, i.e., they converge very slowly and a direct evaluation is impractical if high accuracy is needed.

There are a few systematic techniques in dealing with certain classes of lattice sums. Most significant is that due to Ewald [2], which involves splitting the sums into two parts using a Gaussian truncation function, with one sum over the direct lattice and the other transformed by the Poisson relation to a sum over the reciprocal lattice. Ewald's method is accurate only for low order lattice sums as the Gaussian truncation function is not sufficiently flat at the origin, for high orders, and it is notoriously difficult to find a suitable form for a rapidly converging series [3]. The other commonly used approach is the planewise summation method which, instead of splitting the sums into two parts, separates the fundamental lattice translation vectors into two subsets, with the Poisson formula applied to the sum over the lattice generated by just one of them. The final sum is then taken over a lattice which in some regions is the direct lattice, and in others is the reciprocal lattice [4–7]. It was pointed out that, with some simple guiding rules (usually dictated by the physical constraints of the problem), almost all classes of lattice sums involving a long-range potential can be split into two rapidly converging series (one over the direct lattice and the other over the reciprocal lattice) [8].

Another quite different approach required the exploitation of the symmetry of the lattice to obtain a set of identities between lattice sums, with different carefully chosen origins of coordinates [3]. In this case, the computer implementation of these identities proved much less cumbersome than that of Ewald's method, and could be used for arbitrary high order lattice sums, with good accuracy. However, the absence of square symmetry does not allow us to use this method in problems involving off-axis incident radiation.

Here, we describe an alternative method to express the lattice sums as absolutely converging series. The procedure relies on the relationship between the general two-dimensional Green's function of the direct lattice space and that of the reciprocal lattice space. The Green's functions have to satisfy the periodicity or quasiperiodicity condition for normal incidence or off-axis incidence, respectively. Besides its efficiency, this method also allows us to have some physical insight into the analytical properties of the lattice sums. Moreover, the method also involves some intriguing mathematics which deserves further investigation.

In what follows, we will discuss Green's function and lattice sums in the context of the Rayleigh identity for TM modes. Of course, the Green's function and lattice sums are exactly the same for TE polarization.

We mention that our formulas for the lattice sums lead to fast computer programs to obtain sets of values of the Green's function, for a given set of parameters characterizing the incident radiation.

II. PERIODIC GREEN'S FUNCTION AND LATTICE SUMS FOR NORMAL INCIDENCE

We consider the following diffraction problem: a plane electromagnetic wave is incident normally on a capacitive grid consisting of a square array of perfectly conducting cylinders of radius a and length h. The spatial periodicity of the array is $d = 1$ and the cylinders are separated by free space (see Fig. 1). The incident plane wave is characterized by its wavelength λ and the wave vector:

$$\mathbf{k}^i = -\frac{2\pi}{\lambda}(\sin\varphi\cos\theta, \sin\varphi\sin\theta, \cos\varphi)$$

(for normal incidence $\varphi = 0$).

We use an infinite set of reflected plane waves in the

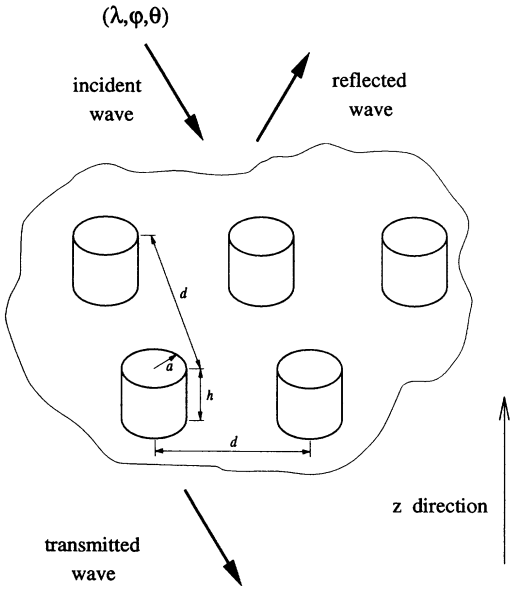

FIG. 1. Electromagnetic diffraction by a doubly periodic array of cylinders.

space $z > h$, and an infinite set of transmitted plane waves in the space $z < 0$. For the TM mode, in the region $0 < z < h$, we express the field as a sum of modes satisfying the two-dimensional Helmholtz equation

$$\Delta_2 V(\mathbf{r}) + k_\perp^2 V(\mathbf{r}) = 0, \tag{1}$$

the boundary condition at the surface of each cylinder

$$V|_{\partial C_p} = 0, \tag{2}$$

and a periodicity condition at the edge of each period cell of the array.

In polar coordinates (ρ, θ, z), around the central cylinder, the modes have the form

$$V(\rho,\theta,z) = \sum_{n=-\infty}^{\infty} [A_n J_n(k_\perp \rho) + B_n Y_n(k_\perp \rho)]\, e^{in\theta} e^{ik_\parallel z} , \tag{3}$$

where $k_\perp$ and $k_\parallel$ are related to the wave vector $\mathbf{k}$ by

$$k^2 = k_\perp^2 + k_\parallel^2 = (2\pi/\lambda)^2 ,$$

and the J_n and Y_n are Bessel functions of the first and second kind.

In (3), the boundary condition (2) implies

$$A_n = -\frac{Y_n(k_\perp a)}{J_n(k_\perp a)} B_n .$$

The Green's function for Eq. (1) is the elementary solution of the inhomogeneous Helmholtz equation

$$\Delta_2 G(\mathbf{r}) + k_\perp^2 G(\mathbf{r}) = -2\pi\delta(\mathbf{r}) , \tag{4}$$

in which $\delta(\mathbf{r})$ is the two-dimensional Dirac function.

Substituting in this equation the Fourier integrals:

$$G(\mathbf{r}) = \int g(\mathbf{k}) e^{i\mathbf{k}\cdot\mathbf{r}} d\mathbf{k} \quad \text{and} \quad \delta(\mathbf{r}) = \frac{1}{(2\pi)^2} \int e^{i\mathbf{k}\cdot\mathbf{r}} d\mathbf{k} ,$$

we obtain [9]

$$G(\mathbf{r}) = \frac{1}{2\pi} \int \frac{e^{i\mathbf{k}\cdot\mathbf{r}}}{k^2 - k_\perp^2} d\mathbf{k} = K_0(-ik_\perp r) = \frac{i\pi}{2} H_0^{(1)}(k_\perp r) . \tag{5}$$

Substituting G and V into Green's theorem and applying the method developed by Lord Rayleigh [1], for the electrostatic problem, we obtain the algebraic system [3]

$$\left[i - \frac{Y_n(k_\perp a)}{J_n(k_\perp a)} \right] B_n + i \sum_{k=-\infty}^{\infty} (-1)^k B_k S_{k+n}(k_\perp) = 0, \tag{6}$$

where S_n are the lattice sums defined as

$$S_n(k_\perp) = \sum_{p \neq 0} H_n^{(1)}(k_\perp R_p) e^{in\varphi_p} . \tag{7}$$

$H_n^{(1)}$ are the Hankel functions and $\mathbf{R}_p = (R_p, \varphi_p)$ are vectors pointing from the origin of coordinates to the center of the pth cylinder. In the derivation of (6) it was assumed that the field (3) is symmetric about $\theta = 0$ [i.e., $B_n = (-1)^n B_{-n}$] and satisfies the periodicity condition

$$V(\mathbf{R}_p + \mathbf{r}) = V(\mathbf{r}) .$$

An algebraic error in [3] causing the omission of a power of (-1) has been corrected in Eq. (6).

A. Periodic Green's function

If we consider the inhomogeneous Helmholtz equation

$$(\Delta_2 + k_\perp^2) G(\mathbf{r}) = -2\pi \sum_p \delta(\mathbf{r} - \mathbf{R}_p) , \tag{8}$$

to define, over the direct lattice, the doubly periodic Green's function

$$G_d(\mathbf{r};\boldsymbol{\rho}) = \frac{i\pi}{2} \sum_p H_0^{(1)}(k_\perp \mid \mathbf{r} - \mathbf{R}_p - \boldsymbol{\rho} \mid) , \tag{9}$$

then the field inside the unit cell, centered at the origin of coordinates, is obtained from Green's theorem by integrating only over the surface of the central cylinder:

$$V(\rho,\theta,z) = -\frac{1}{2\pi} \int_{\partial C_0} G_d(\mathbf{r};\boldsymbol{\rho}) \frac{\partial V}{\partial \mathbf{r}_0} dl_0 . \tag{10}$$

The right side of (8) embodies the periodicity of the total field.

Equally well, we may define a Green's function over the reciprocal lattice. With $d = 1$, the nodes of the direct lattice are defined by the set of vectors

$$\mathbf{R}_p = (R_p, \varphi_p) = (n\mathbf{i} + m\mathbf{j}) \quad , \quad n, m \in \mathbb{Z},$$

while the structure of the reciprocal lattice is determined by the set of vectors

$$\mathbf{K}_h = (K_h, \theta_h) = 2\pi(n\mathbf{i} + m\mathbf{j}) \quad , \quad n, m \in \mathbb{Z},$$

where, $\mathbf{i}$ and $\mathbf{j}$ represent the unit vectors along the x and y axes, respectively.

By means of the vectors $\mathbf{K}_h$, we may construct the Bloch functions $\exp(i\mathbf{K}_h \cdot \mathbf{r})$, which form a complete system. At the same time, these functions are doubly periodic over the direct lattice [10,11]

$$e^{i\mathbf{K}_h \cdot (\mathbf{r}+\mathbf{R}_p)} = e^{i\mathbf{K}_h \cdot \mathbf{r}} \quad , \quad \forall \mathbf{R}_p \ .$$

Using in (8) the expansions in terms of Bloch functions

$$G(\mathbf{r}) = \sum_h g(\mathbf{K}_h) e^{i\mathbf{K}_h \cdot \mathbf{r}} \ ,$$

and

$$\sum_p \delta(\mathbf{r} - \mathbf{R}_p) = \frac{1}{(2\pi)^2} \sum_h e^{i\mathbf{K}_h \cdot \mathbf{r}} \ ,$$

and replacing $\mathbf{r}$ by $\mathbf{r} - \boldsymbol{\rho}$ we obtain the reciprocal lattice representation (G_r) of the Green's function

$$G_r(\mathbf{r}; \boldsymbol{\rho}) = \frac{1}{2\pi} \sum_h \frac{e^{i\mathbf{K}_h \cdot (\mathbf{r}-\boldsymbol{\rho})}}{K_h^2 - k_\perp^2} \ , \tag{11}$$

which, like (9), is doubly periodic in both arguments:

$$G_r(\mathbf{r} + m\mathbf{R}_p; \boldsymbol{\rho} + n\mathbf{R}_p) = G_r(\mathbf{r}; \boldsymbol{\rho}) \quad , \quad \forall m, n \in \mathbb{Z} \ .$$

The two Green's functions (9) and (11) are proportional. To prove this we make use of the relation

$$\sum_h \delta(\mathbf{r} - \mathbf{K}_h) = \frac{1}{(2\pi)^2} \sum_p e^{-i\mathbf{R}_p \cdot \mathbf{r}} \ , \tag{12}$$

which follows from the Poisson summation formula. In (9) we substitute the Fourier representation of Hankel functions [9]

$$\begin{aligned} G_d(\mathbf{r}; \boldsymbol{\rho}) &= \sum_p \frac{1}{2\pi} \int_{-\infty}^{+\infty} dx' \int_{-\infty}^{+\infty} dy' \frac{e^{i\mathbf{r}' \cdot (\mathbf{r}-\boldsymbol{\rho}-\mathbf{R}_p)}}{r'^2 - k_\perp^2} \\ &= \frac{1}{2\pi} \int_{-\infty}^{+\infty} dx' \int_{-\infty}^{+\infty} dy' \frac{e^{i\mathbf{r}' \cdot (\mathbf{r}-\boldsymbol{\rho})}}{r'^2 - k_\perp^2} \left[\sum_p e^{-i\mathbf{R}_p \cdot \mathbf{r}'} \right] \\ &= 2\pi \int_{-\infty}^{+\infty} dx' \int_{-\infty}^{+\infty} dy' \frac{e^{i\mathbf{r}' \cdot (\mathbf{r}-\boldsymbol{\rho})}}{r'^2 - k_\perp^2} \left[\sum_h \delta(\mathbf{r}' - \mathbf{K}_h) \right] \\ &= 2\pi \sum_h \frac{e^{i\mathbf{K}_h \cdot (\mathbf{r}-\boldsymbol{\rho})}}{\mathbf{K}_h^2 - k_\perp^2} . \end{aligned}$$

Consequently, the Green's functions (9) and (11) are related by the formula

$$G_d(\mathbf{r}; \boldsymbol{\rho}) = (2\pi)^2 G_r(\mathbf{r}; \boldsymbol{\rho}) \ . \tag{13}$$

B. Absolutely convergent series for lattice sums

The two forms of Green's function related by (13) provide us an analytic formula for the lattice sums (7).

In the left hand side of (13), using the expression (9), we separate the term for $p = 0$:

$$\frac{i\pi}{2} H_0^{(1)}(k_\perp \mid \mathbf{r} - \boldsymbol{\rho} \mid) + \frac{i\pi}{2} \sum_{p \neq 0} H_0^{(1)}(k_\perp \mid \mathbf{r} - \boldsymbol{\rho} - \mathbf{R}_p \mid) = 2\pi \sum_h \frac{e^{i\mathbf{K}_h \cdot (\mathbf{r}-\boldsymbol{\rho})}}{\mathbf{K}_h^2 - k_\perp^2} \tag{14}$$

and apply the addition theorem for the Hankel functions [12]. Inside the unit cell centered at the origin we have

$$\mid \mathbf{r} - \boldsymbol{\rho} \mid < \mathbf{R}_p \quad , \quad \forall p \neq 0,$$

so that

$$\sum_{p \neq 0} H_0^{(1)}(k_\perp \mid \mathbf{r} - \boldsymbol{\rho} - \mathbf{R}_p \mid) = \sum_{\ell=-\infty}^{\infty} S_\ell(k_\perp) J_\ell(k_\perp \mid \mathbf{r} - \boldsymbol{\rho} \mid) e^{-i\ell\beta} \ , \tag{15}$$

where the S_ℓ are defined in (7) and $\beta = \arg(\mathbf{r} - \boldsymbol{\rho})$ (see Fig. 2).

We assume also $\mid \mathbf{r} \mid < \mid \boldsymbol{\rho} \mid$. Then, applying a second time the addition theorem for the Hankel and Bessel functions, the left hand side of (14) becomes (see Appendix):

$$\frac{i\pi}{2} \sum_{k=-\infty}^{\infty} H_k^{(1)}(k_\perp \rho) J_k(k_\perp r) e^{-ik\psi} e^{ik\theta} + \frac{i\pi}{2} \sum_{\ell,k=-\infty}^{\infty} S_\ell(k_\perp) J_{\ell-k}(k_\perp \rho) J_{-k}(k_\perp r) e^{-ik\psi} e^{i(k-\ell)\theta} \ . \tag{16}$$

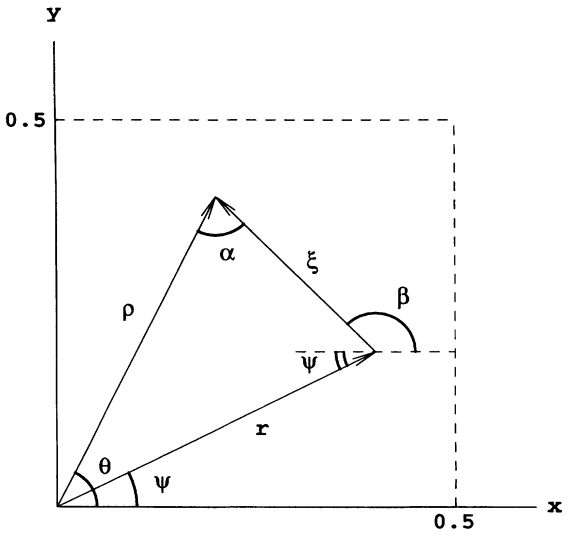

FIG. 2. The geometry for the application of the addition theorem within the unit cell.

In the right hand side of (14) we expand the exponential in terms of Bessel functions [12]:

$$e^{i\mathbf{K}_h\cdot(\mathbf{r}-\boldsymbol{\rho})} = \sum_{n=-\infty}^{\infty} i^n J_n(K_h \mid \mathbf{r}-\boldsymbol{\rho} \mid) e^{in\theta_h} e^{-in\beta} ,$$

and apply the addition theorem for the Bessel functions ($\mid \mathbf{r} \mid < \mid \boldsymbol{\rho} \mid$). Finally, we obtain

$$2\pi \sum_{n,m=-\infty}^{\infty} \sum_h \frac{J_{n-m}(K_h\rho)J_{-m}(K_h r)}{K_h^2 - {k_\perp}^2} \times i^n e^{in\theta_h} e^{-im\psi} e^{i(m-n)\theta} . \quad (17)$$

By equating the coefficients of equal powers of $\exp(i\psi)$ and $\exp(i\theta)$, changing k into $-k$, we obtain from (16) and (17) the set of equations

$$S_\ell(k_\perp)J_{\ell+k}(k_\perp\rho)J_k(k_\perp r) = -H_k^{(1)}(k_\perp\rho)J_k(k_\perp r)\delta_{\ell,0} - 4i^{\ell+1} \sum_h \frac{J_{\ell+k}(K_h\rho)J_k(K_h r)}{K_h^2 - {k_\perp}^2} e^{i\ell\theta_h} . \quad (18)$$

Here, $\delta_{\ell,0}$ denotes the Kronecker symbol and, for fixed $(k_\perp, \ell)$, the equations are independent of (k, ρ, r), provided $\mid \mathbf{r}-\boldsymbol{\rho} \mid < \mathbf{R}_p$ and $\mid \mathbf{r} \mid < \mid \boldsymbol{\rho} \mid$.

This is a remarkable identity relating sums of Bessel functions. It contains free parameters ρ and r (distances within the unit cell) and k (an arbitrary integer).

The fourfold symmetry of the square array implies $S_\ell = 0$ if ℓ is not a multiple of four, and considering the parts of $S_{4\ell}$ in (7) associated with the Bessel functions J and Y separately:

$$S_{4\ell}(k_\perp) = S_{4\ell}^J(k_\perp) + iS_{4\ell}^Y(k_\perp) , \quad (19)$$

we obtain from (18)

$$S_{4\ell}^J(k_\perp) = -\delta_{\ell,0} . \quad (20)$$

For $S_{4\ell}^Y$ we obtain the formula

$$S_{4\ell}^Y(k_\perp)J_{4\ell+k}(k_\perp\rho)J_k(k_\perp r) = -Y_k(k_\perp\rho)J_k(k_\perp r)\delta_{\ell,0} - 4\sum_h \frac{J_{4\ell+k}(K_h\rho)J_k(K_h r)}{K_h^2 - {k_\perp}^2} \cos(4\ell\theta_h) . \quad (21)$$

We multiply both sides of (21) by $\exp[ik(\theta-\psi)]$ and sum over k. The addition theorem for Bessel functions leads us to the formula:

$$S_{4\ell}^Y(k_\perp)J_{4\ell}(k_\perp\xi) = -Y_0(k_\perp\xi)\delta_{\ell,0} - 4\sum_h \frac{J_{4\ell}(K_h\xi)}{K_h^2 - {k_\perp}^2} \cos(4\ell\theta_h) , \quad (22)$$

where $\xi = \mid \boldsymbol{\rho} - \mathbf{r} \mid$. Again, for fixed $(k_\perp, \ell)$, this equation is independent of ξ and provide us an identity relating sums of Bessel functions.

Within the unit cell, $\xi \in (0,1)$, we multiply both sides of (22) by $\xi^{4\ell+1}$ and integrate over ξ. For $\ell \geq 0$, all the integrals may be evaluated in closed form [12]

$$\int_0^1 \xi^{4\ell+1} J_{4\ell}(k_\perp\xi)d\xi = \frac{J_{4\ell+1}(k_\perp)}{k_\perp} ,$$
$$\int_0^1 \xi^{4\ell+1} Y_{4\ell}(k_\perp\xi)d\xi = \frac{Y_{4\ell+1}(k_\perp)}{k_\perp} + \frac{2^{4\ell+1}(4\ell)!}{\pi {k_\perp}^{4\ell+2}} ,$$

and we obtain

$$S_{4\ell}^Y(k_\perp)J_{4\ell+1}(k_\perp) = -\left[Y_1(k_\perp) + \frac{2}{\pi k_\perp}\right]\delta_{\ell,0} - 4k_\perp \sum_h \frac{J_{4\ell+1}(K_h)}{K_h(K_h^2 - {k_\perp}^2)} \cos(4\ell\theta_h) . \quad (23)$$

In the series from the right hand side, the term for $\mathbf{K}_h = \mathbf{0}$ gives a nonzero contribution only if $\ell = 0$. We separate this term and add it to the first part of the right hand side in (23). Finally, we obtain for $S_{4\ell}^Y$ the expression

$$S_{4\ell}^Y(k_\perp)J_{4\ell+1}(k_\perp) = -\left[Y_1(k_\perp) + \left(\frac{2}{\pi} - 2\right)\frac{1}{k_\perp}\right]\delta_{\ell,0} - 4k_\perp \sum_{h\neq 0} \frac{J_{4\ell+1}(K_h)}{K_h(K_h^2 - {k_\perp}^2)} \cos(4\ell\theta_h), \quad (24)$$

which depends on $k_\perp$ only.

For $\ell \leq -1$, the lattice sums are given by relation

$$S_{4\ell}^Y(k_\perp) = S_{-4\ell}^Y(k_\perp) ,$$

which results from (22).

The equation (18) is valid for any ℓ, i.e., with no restriction imposed by the symmetry of the lattice. The

same method leads us to the general expressions

$$S_\ell(k_\perp)J_\ell(k_\perp\xi) = -H_0^{(1)}(k_\perp\xi)\delta_{\ell,0} - 4i^{\ell+1}\sum_h \frac{J_\ell(K_h\xi)}{K_h^2 - {k_\perp}^2}e^{i\ell\theta_h} , \quad (25)$$

and

$$S_\ell(k_\perp) = -\left\{1 + \frac{i}{J_1(k_\perp)}\left[Y_1(k_\perp) + \left(\frac{2}{\pi} - 2\right)\frac{1}{k_\perp}\right]\right\}\delta_{\ell,0} - i^{\ell+1}\frac{4k_\perp}{J_{\ell+1}(k_\perp)}\sum_{h\neq 0}\frac{J_{\ell+1}(K_h)}{K_h(K_h^2 - {k_\perp}^2)}e^{i\ell\theta_h} , \quad (26)$$

valid, with the corresponding changes in the definitions of $\mathbf{R}_p$ and $\mathbf{K}_h$, for any regular two-dimensional lattice. Here, we have employed the relation

$$\int_0^1 \xi^{n+1}H_n^{(1,2)}(k_\perp\xi)d\xi = \frac{H_{n+1}^{(1,2)}(k_\perp)}{k_\perp} \pm i\frac{2^{n+1}\,n!}{\pi {k_\perp}^{n+2}} ,$$

for $n \geq 0$. Again, the lattice sums of negative order are obtained from the corresponding lattice sums of positive order by means of (25).

C. Comments on the lattice sums expressions and relation to the previous work

The series involved in the equation (24) converge as $K_h^{-3.5}$ for large K_h, whereas the corresponding series (21,22) converge as K_h^{-3} and $K_h^{-2.5}$, respectively. In fact, all these series become more slowly convergent in the neighborhood of a root of those Bessel functions depending on $k_\perp$. We discuss later a technique which enables us to avoid problems in the neighborhood of such roots.

Numerical values of the lattice sums $S_{4\ell}^Y(k_\perp)$, obtained from (24), generate curves which coincide exactly with the curves determined numerically by Ewald's method or the lattice sum identity in Ref. [3] (see Fig. 3). More precisely, some of these numerical results are presented in Tables I and II. It can be seen in Table I that the maximum relative error between the results from [3] and Eq. (24) occurs at the points close to a root of $J_{4\ell+1}(k_\perp)$. In all these cases the relative error becomes significantly smaller by applying l'Hôpital's rule, or the technique described in Sec. III B.

A main characteristic of the formulas (21,22,24) is that the involved series are absolutely convergent, in contrast to the definition (7) where the series are conditionally convergent.

From (24) we deduce the behavior of the lattice sums for small $k_\perp$. If $\ell \neq 0$ we have

$$S_{4\ell}^Y(k_\perp) \sim -\frac{2^{4\ell+3}(4\ell+1)!}{{k_\perp}^{4\ell}}\sum_{h\neq 0}\frac{J_{4\ell+1}(K_h)}{K_h^3}\cos(4\ell\theta_h) \sim -\frac{1}{{k_\perp}^{4\ell}} , \quad (27)$$

while for $\ell = 0$

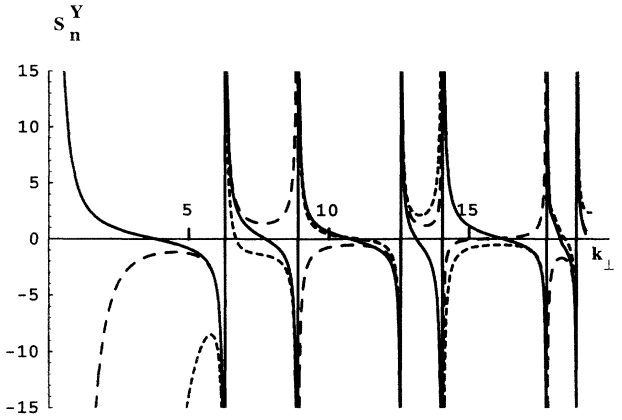

FIG. 3. Normal incidence. The variations of the first three nonzero lattice sums with $k_\perp$ are shown, with the solid curve for S_0^Y, coarse-dashed curve for S_4^Y, and fine-dashed curve for S_8^Y.

$$S_0^Y(k_\perp) \sim \frac{4}{{k_\perp}^2} - \frac{2}{\pi}\ln\left(\frac{k_\perp}{2}\right) + \frac{1-2\gamma}{\pi} - 8\sum_{h\neq 0}\frac{J_1(K_h)}{K_h^3} , \quad (28)$$

where $\gamma \simeq 0.577216$ denotes Euler's constant. The numerical value of the last term is

$$8\sum_{h\neq 0}\frac{J_1(K_h)}{K_h^3} \simeq -1.600128 \times 10^{-2}.$$

All the lattice sums exhibit a simple pole if $k_\perp$ equals the magnitude K of a reciprocal lattice vector. The behavior close to such a point ($K \neq 0$) is given by the formula

$$S_{4\ell}^Y(k_\perp) \sim \frac{4}{{k_\perp}^2 - K^2}\sum_{\mathbf{K}_i}\cos(4\ell\theta_i) , \quad (29)$$

where the sum is over all reciprocal lattice vectors $\mathbf{K}_i = (K, \theta_i)$. The fourfold symmetry of the reciprocal lattice introduces a degeneracy of poles. For every pair of integers, (n, m), excepting $(0, 0)$, we have four vectors $\mathbf{K}_i$ of the same magnitude and the sum in (29) contains four terms. This formula also applies to S_0^Y.

The results (27)–(29) were also obtained in Ref. [3] by a different technique. We mention that the method presented here allows us to obtain a more complete expression for the behavior of $S_0^Y(k_\perp)$ for small $k_\perp$.

The sign of $\sum\cos(4\ell\theta_i)$, in (29), determines the way $S_{4\ell}^Y(k_\perp)$ tends to infinity at the right and left hand side of a pole. All the poles are simple and consequently, Eq. (29) controls the shape of the curves between two successive poles (see Fig. 3). If at the ends of the interval between two succesive poles $S_{4\ell}^Y(k_\perp)$ has different signs, then the shape of the corresponding curve, in this interval, is cotangentlike (one inflexion point and one zero). If at both the ends of the interval $S_{4\ell}^Y(k_\perp)$ has the same sign, the shape is parabolalike (one point of extremum and two, one, or no zeros).

Among the set of lattice sums $S^Y_{4\ell}(k_\perp)$ only $S^Y_0(k_\perp)$ is monotonically decreasing in all the intervals between two successive poles. Excepting the origin ($k_\perp = 0$), which is an essential singularity generated by the logarithmic term in (28), $S^Y_0(k_\perp)$ has only simple, alternating poles and zeros. For $\ell \geq 1$, the lattice sums $S^Y_{4\ell}(k_\perp)$ exibit a pole of order 4ℓ at the origin and simple poles in the range $k_\perp \in (0, \infty)$. For lattice sums of all order, $k_\perp = \infty$ is an accumulation point of poles, i.e., an essential singularity. We may conclude that the Eqs. (20) and (24) provide a good analytic representation of the lattice sums $S_{4\ell}(k_\perp)$ for a square lattice.

Generally, we may assert the following:

(a) All the poles of $S^Y_{4\ell}$ are the same as the poles of the right hand side of (24) and vice versa, being located at the points $k_\perp = K_h$.

(b) The zeros of $S^Y_{4\ell}$ are the same as the zeros of the right hand side of (24) unless $k_\perp$ equals a zero of $J_{4\ell+1}$,when a detailed analysis is required.

(c) If $J_{4\ell+1}(x_0) = 0$ then, at the point x_0, the right hand side of (24) vanishes, provided x_0 does not equal the magnitude of one reciprocal lattice vector. Consequently, for $k_\perp = x_0 \neq K_h$, we may apply l'Hôpital's rule, or the technique discussed in Sec. III B. L'Hôpital's rule gives

$$S^Y_{4\ell}(x_0)J_{4\ell+2}(x_0) = -\left[Y_2(x_0) + \left(\frac{1}{\pi} - 1\right)\frac{4}{x_0^2}\right]\delta_{\ell,0} + 8x_0^2 \sum_{h\neq 0} \frac{J_{4\ell+1}(K_h)}{K_h(K_h^2 - x_0^2)^2} \cos(4\ell\theta_h) \ , \tag{30}$$

where the series converge as $K_h^{-5.5}$. The zeros of $J_{4\ell+1}(z)$ and $J_{4\ell+2}(z)$ separate each other [13]. Therefore, $J_{4\ell+2}(x_0) \neq 0$ and (30) determines the value of $S^Y_{4\ell}(x_0)$.

TABLE I. Numerical values of $S^Y_0(k_\perp)$ as given in Ref. [3] and by Eq. (23), summed over a square array of 201 by 201 cylinders. The last column represents the right hand side (rhs) of (23) at the points where $J_1(k_\perp) = 0$.

$k_\perp$	Ref. [3]	Eq. (23)	Relative error	Roots of $J_1(k_\perp) = 0$	rhs (23)
2	1.399 630	1.399 630	0		
2.994 97	0.486 082	0.486 082	0		
3.809 04	0.010 712	0.010 711	0.000 062 772		
				3.831 706	$-2.576\,89 \times 10^{-8}$
3.899 5	−0.040 071	−0.040 071	$5.670\,95 \times 10^{-6}$		
4.984 92	−0.807 882	−0.807 882	0		
5.979 9	−4.293 390	−4.293 390	0		
6.974 87	1.417 760	1.417 760	$4.204\,15 \times 10^{-7}$		
				7.015 587	$1.181\,14 \times 10^{-7}$
7.065 33	1.166 760	1.166 760	$5.108\,54 \times 10^{-7}$		
7.969 85	−0.342 809	−0.342 809	$1.738\,71 \times 10^{-7}$		
8.964 82	11.571 000	11.571 000	0		
10.140 7	0.487 108	0.487 105	$5.873\,49 \times 10^{-6}$		
				10.173 468	$-7.401\,97 \times 10^{-8}$
10.231 2	0.405 418	0.405 420	$4.116\,57 \times 10^{-6}$		
10.954 8	−0.141 872	−0.141 872	$1.155\,36 \times 10^{-6}$		
11.949 7	−1.244 500	−1.244 500	$9.578\,87 \times 10^{-8}$		
12.944 7	0.765 385	0.765 385	$4.672\,52 \times 10^{-7}$		
13.306 5	−0.631 232	−0.631 264	0.000 013 314		
				13.323 692	$-9.778\,29 \times 10^{-8}$
13.397	−0.955 180	−0.955 182	$2.059\,25 \times 10^{-6}$		
13.939 7	−9.980 070	−9.980 070	0		
14.934 7	1.259 090	1.259 090	$1.893\,58 \times 10^{-7}$		
15.929 7	0.260 733	0.260 732	$2.025\,23 \times 10^{-6}$		
16.381 9	−0.103 075	−0.103 077	0.000 026 769		
				16.470 630	$-9.302\,67 \times 10^{-9}$
16.472 4	−0.170 700	−0.172 018	0.007 726 5		
16.562 8	−0.241 093	−0.241 091	$9.580\,02 \times 10^{-6}$		
16.924 6	−0.576 857	−0.576 857	$8.266\,12 \times 10^{-7}$		
17.919 6	2.370 490	2.370 490	$1.005\,78 \times 10^{-7}$		
18.914 6	6.062 670	6.062 670	$7.865\,66 \times 10^{-8}$		
19.547 7	−1.799 320	−1.799 320	$2.385\,08 \times 10^{-6}$		
				19.615 859	$-4.113\,42 \times 10^{-7}$
19.638 2	−2.883 320	−2.883 330	$4.630\,58 \times 10^{-6}$		
20	6.461 610	6.461 610	$1.475\,91 \times 10^{-7}$		

TABLE II. Numerical values of $S^Y_{12}(k_\perp)$ as given in Ref. [3] and by Eq. (23), summed over a square array of 201 by 201 cylinders, together with the nearest-neighbors estimate $4Y_{12}(k_\perp)$. The last two columns display $S^Y_{24}(k_\perp)$ together with the nearest-neighbors estimate.

$k_\perp$	Ref. [3]	Eq. (23)	Relative error	$4Y_{12}(k_\perp)$	$S^Y_{24}(k_\perp)$	$4Y_{24}(k_\perp)$
2	$-5.475\,52 \times 10^7$	$-5.475\,50 \times 10^7$	$2.995\,15 \times 10^{-6}$	$-5.568\,38 \times 10^7$	$-3.438\,88 \times 10^{22}$	$-3.438\,00 \times 10^{22}$
2.994 97	$-4.819\,68 \times 10^5$	$-4.819\,66 \times 10^5$	$2.917\,73 \times 10^{-6}$	$-4.911\,05 \times 10^5$	$-2.245\,14 \times 10^{18}$	$-2.244\,53 \times 10^{18}$
3.989 95	$-1.809\,01 \times 10^4$	$-1.809\,00 \times 10^4$	$2.807\,13 \times 10^{-6}$	$-1.849\,09 \times 10^4$	$-2.480\,17 \times 10^{15}$	$-2.479\,45 \times 10^{15}$
4.984 92	−1541.740 000	−1541.730 000	$2.692\,02 \times 10^{-6}$	−1582.677 862	$-1.307\,66 \times 10^{13}$	$-1.307\,24 \times 10^{13}$
5.979 9	−269.332 000	−269.331 000	$2.528\,36 \times 10^{-6}$	−233.113 429	$-1.870\,52 \times 10^{11}$	$-1.869\,84 \times 10^{11}$
6.974 87	−46.704 800	−46.704 700	$2.531\,98 \times 10^{-6}$	−51.152 084	$-5.369\,62 \times 10^9$	$-5.367\,35 \times 10^9$
7.969 85	−12.887 900	−12.887 900	$2.441\,92 \times 10^{-6}$	−15.462 449	$-2.584\,12 \times 10^8$	$-2.582\,81 \times 10^8$
8.964 82	−16.659 600	−16.659 600	$5.724\,46 \times 10^{-7}$	−6.193 760	$-1.856\,80 \times 10^7$	$-1.855\,64 \times 10^7$
9.959 8	−3.428 720	−3.428 720	$1.251\,64 \times 10^{-6}$	−3.208 700	$-1.841\,10 \times 10^6$	$-1.839\,64 \times 10^6$
10.954 8	−2.169 510	−2.169 500	$9.890\,58 \times 10^{-7}$	−2.030 871	$-2.382\,25 \times 10^5$	$-2.379\,75 \times 10^5$
11.949 7	−2.315 210	−2.315210	$6.178\,76 \times 10^{-7}$	−1.382 722	$-3.861\,70 \times 10^4$	$-3.855\,98 \times 10^4$
12.944 7	0.352 599	0.352 600	$2.451\,13 \times 10^{-6}$	−0.816 185	$-7.605\,01 \times 10^3$	$-7.590\,29 \times 10^3$
13.939 7	−7.691 110	−7.691110	$1.239\,97 \times 10^{-7}$	−0.197076	$-1.780\,38 \times 10^3$	$-1.773\,46 \times 10^3$
14.934 7	1.014 000	1.014 000	$5.878\,17 \times 10^{-7}$	0.416 306	$-4.856\,18 \times 10^2$	$-4.832\,15 \times 10^2$
15.929 7	0.563 684	0.563 684	$1.480\,38 \times 10^{-6}$	0.845 771	$-1.529\,82 \times 10^2$	$-1.515\,06 \times 10^2$
16.924 6	0.664 173	0.664 174	$2.333\,31 \times 10^{-6}$	0.907 907	$-5.551\,42 \times 10^1$	$-5.414\,34 \times 10^1$
17.919 6	−3.123 000	−3.123 010	$3.740\,80 \times 10^{-6}$	0.551 578	$-1.973\,35 \times 10^1$	$-2.192\,63 \times 10^1$
18.914 6	6.768 980	6.768 980	$2.113\,33 \times 10^{-7}$	−0.061 269	−3.424 13	$-1.004\,57 \times 10^1$
20	−4.537 380	−4.537 380	$3.152\,73 \times 10^{-7}$	−0.639 009	−3.651 84	−4.949 85

In addition, the high order lattice sums are usefully approximated for $k_\perp < 2\ell$, by the formula [3]

$$S^Y_{4\ell}(k_\perp) \sim 4Y_{4\ell}(k_\perp) \ . \tag{31}$$

A numerical example illustrating this approximation is given in Table II. Note that the approximation (31), for large ℓ, is accurate presque partout (p.p.), isolated exceptional points such as the poles of $S^Y_{4\ell}$ being excluded.

III. QUASIPERIODIC GREEN'S FUNCTION AND LATTICE SUMS FOR OFF-AXIS INCIDENCE

A. Quasiperiodic Green's function

For the off-axis incidence we use the complete set of Bloch functions

$$\psi_h(\mathbf{r}) = e^{i\left(\mathbf{K}_h + \mathbf{k}^i_\perp\right)\cdot\mathbf{r}} \ , \tag{32}$$

satisfying the quasiperiodicity condition:

$$\psi_h(\mathbf{r} + \mathbf{R}_p) = e^{i\mathbf{k}^i_\perp\cdot\mathbf{R}_p}\ \psi_h(\mathbf{r}) \ . \tag{33}$$

Here, $\mathbf{k}^i_\perp$ represents the projection of the incident wave vector $\mathbf{k}^i$, onto the xy plane.

To account for the quasiperiodicity condition the Helmholtz equation (8) becomes

$$(\Delta_2 + k_\perp^2)G_d(\mathbf{r}) = -2\pi \sum_p \delta(\mathbf{r} - \mathbf{R}_p)\ e^{i\mathbf{k}^i_\perp\cdot\mathbf{R}_p} \ , \tag{34}$$

in the direct lattice space, and

$$(\Delta_2 + k_\perp^2)G_r(\mathbf{r}) = -\frac{1}{2\pi}\sum_h \psi_h(\mathbf{r}) \ , \tag{35}$$

in the reciprocal lattice space. The solutions of these two equations are related by the formula

$$G_d(\mathbf{r}) = (2\pi)^2 G_r(\mathbf{r}) \ , \tag{36}$$

the same as (13). Here, to prove this, we use the relations

$$\begin{aligned}\sum_h \psi_h(\mathbf{r}) &= e^{i\mathbf{k}^i_\perp\cdot\mathbf{r}} \sum_h e^{i\mathbf{K}_h\cdot\mathbf{r}} \\ &= e^{i\mathbf{k}^i_\perp\cdot\mathbf{r}} \left[(2\pi)^2 \sum_p \delta(\mathbf{r} - \mathbf{R}_p)\right] \\ &= (2\pi)^2 \sum_p \delta(\mathbf{r} - \mathbf{R}_p)\ e^{i\mathbf{k}^i_\perp\cdot\mathbf{R}_p} \ .\end{aligned}$$

The two Green's functions are quasiperiodic:

$$G_{d,r}(\mathbf{r} + \mathbf{R}_p) = \ e^{i\mathbf{k}^i_\perp\cdot\mathbf{R}_p}\ G_{d,r}(\mathbf{r}) \ , \tag{37}$$

and, in the direct lattice space, we have

$$G_d(\mathbf{r};\boldsymbol{\rho}) = \frac{i\pi}{2}\sum_p H_0^{(1)}(k_\perp \mid \mathbf{r} - \mathbf{R}_p - \boldsymbol{\rho} \mid)\, e^{i\mathbf{k}^i_\perp\cdot\mathbf{R}_p}. \tag{38}$$

From (35) we obtain the Green's function in the reciprocal lattice space:

$$G_r(\mathbf{r};\boldsymbol{\rho}) = \frac{1}{2\pi}\sum_h \frac{e^{i\mathbf{Q}_h\cdot(\mathbf{r}-\boldsymbol{\rho})}}{Q_h^2 - k_\perp^2} \ , \tag{39}$$

where $\mathbf{Q}_h = \mathbf{K}_h + \mathbf{k}^i_\perp$.

We apply the same method as in Sec. II A using solution (3) and integrating only over the surface of the central cylinder. For a TM mode, the Rayleigh method leads us to the linear system [$\tilde{B}_n = (-1)^n B_{-n}$]:

$$\left[i - \frac{Y_n(k_\perp a)}{J_n(k_\perp a)}\right] \tilde{B}_n + i \sum_{k=-\infty}^{\infty} \tilde{B}_{-k} \mathcal{S}_{k+n}(k_\perp) = 0 \ . \qquad (40)$$

Now, the lattice sums $\mathcal{S}_\ell$ are given by the formula

$$\mathcal{S}_\ell(k_\perp) = \sum_{p \neq 0} H_\ell^{(1)}(k_\perp R_p)\ e^{i\ell\varphi_p}\ e^{i\mathbf{k}_\perp^i \cdot \mathbf{R}_p} \ . \qquad (41)$$

B. Absolutely convergent lattice sum expressions

We split the lattice sums (41) into two parts, pointing out the series involving the Bessel functions J and Y:

$$\mathcal{S}_\ell^J(k_\perp) = \sum_{p \neq 0} J_\ell(k_\perp R_p)\ e^{i\ell\varphi_p}\ e^{i\mathbf{k}_\perp^i \cdot \mathbf{R}_p} \qquad (42)$$

and

$$\mathcal{S}_\ell^Y(k_\perp) = \sum_{p \neq 0} Y_\ell(k_\perp R_p)\ e^{i\ell\varphi_p}\ e^{i\mathbf{k}_\perp^i \cdot \mathbf{R}_p} \ , \qquad (43)$$

so that

$$\mathcal{S}_\ell(k_\perp) = \mathcal{S}_\ell^J(k_\perp) + i\mathcal{S}_\ell^Y(k_\perp) \ . \qquad (44)$$

In contrast with the case of normal incidence, for off-axis incidence, in general, both $\mathcal{S}_\ell^J$ and $\mathcal{S}_\ell^Y$ are complex, and $\mathcal{S}_\ell$ of all orders are nonzero. This means that (44) is not a separation into the real and imaginary parts of $\mathcal{S}_\ell$.

First, we consider the lattice sums $\mathcal{S}_\ell^J$, defined in (42). The Poisson summation formula relates the vectors from the direct and reciprocal lattices:

$$\sum_p e^{-i\mathbf{r}\cdot\mathbf{R}_p} = (2\pi)^2 \sum_h \delta(\mathbf{r} - \mathbf{K}_h) \ ,$$

for all vectors $\mathbf{r}$ in the lattice plane. By defining $\boldsymbol{r} = \mathbf{k}_\perp - \mathbf{k}_\perp^i$, we obtain

$$\sum_p e^{-i(\mathbf{k}_\perp - \mathbf{k}_\perp^i)\cdot\mathbf{R}_p} = 0 \ ,$$

unless $\mathbf{k}_\perp - \mathbf{k}_\perp^i$ equals any of the reciprocal lattice vector $\mathbf{K}_h$. In this formula, we substitute the expansion [12]

$$e^{-i\mathbf{k}_\perp\cdot\mathbf{R}_p} = e^{-ik_\perp R_p \cos(\theta_\perp - \varphi_p)} = \sum_{n=-\infty}^{\infty} (-i)^n J_n(k_\perp R_p) e^{in\varphi_p} e^{-in\theta_\perp} \ ,$$

multiply both sides by $\exp(i\ell\theta_\perp)$ and integrate with respect to $\theta_\perp$ from 0 to 2π. Finally, with the definition (42) and the relation $J_\ell(0) = \delta_{\ell,0}$, we get

$$\mathcal{S}_\ell^J(k_\perp) = -\delta_{\ell,0} \ , \qquad (45)$$

i.e., the same result as (20). This means that the lattice sums $\mathcal{S}_\ell^J$ take the same values independent of the direction of the incident radiation.

To obtain the expression of $\mathcal{S}_\ell^Y$, we substitute (38) and (39) in (36):

$$\frac{i\pi}{2} H_0^{(1)}(k_\perp \mid \mathbf{r} - \boldsymbol{\rho} \mid) + \frac{i\pi}{2} \sum_{p \neq 0} H_0^{(1)}(k_\perp \mid \mathbf{r} - \boldsymbol{\rho} - \mathbf{R}_p \mid) e^{i\mathbf{k}_\perp^i \cdot \mathbf{R}_p} = 2\pi \sum_h \frac{e^{i\mathbf{Q}_h\cdot(\mathbf{r}-\boldsymbol{\rho})}}{\mathbf{Q}_h^2 - k_\perp^2} \ , \qquad (46)$$

where the term with $p = 0$ is separated out from the series. As in the case of normal incidence, we apply the addition theorem for Hankel functions, assuming that $\mathbf{r}$ and $\boldsymbol{\rho}$ are restricted to the central unit cell. The series in the left side of (46) becomes

$$\sum_{p \neq 0} H_0^{(1)}(k_\perp \mid \mathbf{r} - \boldsymbol{\rho} - \mathbf{R}_p \mid) e^{i\mathbf{k}_\perp^i \cdot \mathbf{R}_p} = \sum_{\ell=-\infty}^{\infty} \mathcal{S}_\ell(k_\perp) J_\ell(k_\perp \xi) e^{-i\ell\beta} \ . \qquad (47)$$

Then, we expand the exponential, in the right hand side of (46), in terms of Bessel functions with the argument $Q_h\xi$, and equate the coefficients of equal powers of $\exp(-i\beta)$. This, leads us to the set of equations

$$\mathcal{S}_\ell(k_\perp) J_\ell(k_\perp \xi) = -H_0^{(1)}(k_\perp \xi)\delta_{\ell,0} - 4i^{\ell+1} \sum_h \frac{J_\ell(Q_h\xi)}{Q_h^2 - {k_\perp}^2} e^{i\ell\theta_h} \ , \qquad (48)$$

where $\mathbf{Q}_h = (Q_h, \theta_h)$. By substituting (45) into (48) we have

$$\mathcal{S}_\ell^Y(k_\perp) J_\ell(k_\perp \xi) = -Y_0(k_\perp \xi)\delta_{\ell,0} - 4i^\ell \sum_h \frac{J_\ell(Q_h\xi)}{Q_h^2 - {k_\perp}^2} e^{i\ell\theta_h} \ . \qquad (49)$$

Further, following the same method as in Sec. II B, i.e., multiplying both sides of (49) by $\xi^{\ell+1}$ and integrating over ξ from 0 to 1, we obtain, for $\ell > -1$

$$\mathcal{S}_\ell^Y(k_\perp) J_{\ell+1}(k_\perp) = -\left[Y_1(k_\perp) + \frac{2}{\pi k_\perp}\right] \delta_{\ell,0} - 4i^\ell k_\perp \sum_h \frac{J_{\ell+1}(Q_h)}{Q_h(Q_h^2 - {k_\perp}^2)} e^{i\ell\theta_h} \ . \qquad (50)$$

We may improve the convergence rate of the series in (50), if we introduce a parameter $\eta < 1$ and integrate (49), multiplied by $\xi^{\ell+1}$, from 0 to η. In this case, the integrals take the forms [12]

$$\int_0^\eta \xi^{\ell+1} J_\ell(k_\perp \xi)\, d\xi = \eta^{\ell+1} \frac{J_{\ell+1}(k_\perp \eta)}{k_\perp} \ ,$$

$$\int_0^\eta \xi^{\ell+1} Y_\ell(k_\perp \xi)\, d\xi = \eta^{\ell+1} \frac{Y_{\ell+1}(k_\perp \eta)}{k_\perp} + \frac{2^{\ell+1}(\ell)!}{\pi {k_\perp}^{\ell+2}} \ ,$$

and we obtain

$$\mathcal{S}_\ell^Y(k_\perp)J_{\ell+1}(k_\perp\eta) = -\left[Y_1(k_\perp\eta)+\frac{2}{\pi\eta k_\perp}\right]\delta_{\ell,0} - 4i^\ell\sum_h\left(\frac{k_\perp}{Q_h}\right)\frac{J_{\ell+1}(Q_h\eta)}{Q_h^2-{k_\perp}^2}\,e^{i\ell\theta_h}. \tag{51}$$

Now we change η into ξ and repeat the same procedure. After m steps we have

$$\mathcal{S}_\ell^Y(k_\perp)J_{\ell+m}(k_\perp\eta) = -\left[Y_m(k_\perp\eta)+\frac{1}{\pi}\sum_{k=1}^{m}\frac{(m-k)!}{(k-1)!}\left(\frac{2}{k_\perp\eta}\right)^{m-2k+2}\right]\delta_{\ell,0} - 4i^\ell\sum_h\left(\frac{k_\perp}{Q_h}\right)^m\frac{J_{\ell+m}(Q_h\eta)}{Q_h^2-{k_\perp}^2}\,e^{i\ell\theta_h}\ , \tag{52}$$

and, by substituting $\eta = 1$, we obtain a new formula with a series converging as $Q_h^{-m-2.5}$. The parameter m is arbitrary. If we increase m, we improve the convergence, but too large values of m lead to problems of numerical stability. This is, particularly, the case for $k_\perp$ small, when indeed (49), with $\xi = 1$, may be preferable to (52).

For (22), the same method gives

$$S_{4\ell}^Y(k_\perp)J_{4\ell+m}(k_\perp\eta) = -\left[Y_m(k_\perp\eta)+\frac{1}{\pi}\sum_{k=1}^{m}\frac{(m-k)!}{(k-1)!}\left(\frac{2}{k_\perp\eta}\right)^{m-2k+2} -\frac{4}{{k_\perp}^2}\frac{(k_\perp\eta)^m}{2^m m!}\right]\delta_{\ell,0} -4\sum_{h\neq0}\left(\frac{k_\perp}{K_h}\right)^m\frac{J_{4\ell+m}(K_h\eta)}{K_h^2-{k_\perp}^2}\cos(4\ell\theta_h)\ . \tag{53}$$

Note the difference between (52) and (53) regarding the involved series, namely, in (53) the term for $h = 0$ is omitted in the series and generates an extra term in the coefficient of $\delta_{\ell,0}$.

The formulas (52) and (53) may be used instead of l'Hôpital's rule; when $k_\perp$ approaches a zero of the Bessel function we have to use the corresponding formula for $m+1$.

C. Analytical properties of the lattice sums

Generally, in the case of oblique incidence, from (43), we have

$$\mathcal{S}_{-\ell}^Y(k_\perp) = \mathcal{S}_\ell^{Y*}(k_\perp)\ ,$$

and the lattice sums $\mathcal{S}_\ell^Y$ are complex for all ℓ, except $\mathcal{S}_0^Y$ which remains real in all cases. These equations have to be used for negative values of ℓ, as (50) and (52) are valid for $\ell > -1$ only.

From (50) we deduce the behavior of the lattice sums for small $k_\perp$. If $\ell \neq 0$ the origin is a pole of order ℓ:

$$S_\ell^Y(k_\perp) \sim -\frac{2^{\ell+3}(\ell+1)!}{{k_\perp}^\ell}\,i^\ell\sum_h\frac{J_{\ell+1}(Q_h)}{Q_h^3}\,e^{i\ell\theta_h} \sim -\frac{1}{{k_\perp}^\ell}\ ; \tag{54}$$

while, for $\ell = 0$ the origin is an essential singularity:

$$S_0^Y(k_\perp) \sim -\frac{2}{\pi}\ln\left(\frac{k_\perp}{2}\right)+\frac{1-2\gamma}{\pi} -8\frac{J_1(k_i)}{k_i(k_i^2-k_\perp^2)} - 8\sum_{h\neq0}\frac{J_1(Q_h)}{Q_h^3}\ . \tag{55}$$

Here, in contrast to (27) and (28), Q_h depends on $\mathbf{k}_\perp^i$. Note that, as $|\mathbf{k}_\perp^i| \equiv k_i \to 0$, the result (55) approaches (28).

The set of vectors $\{\mathbf{Q}_h\}$ defines a lattice obtained from the reciprocal lattice $\{\mathbf{K}_h\}$ by a translation of $\mathbf{k}_\perp^i$. All the lattice sums exhibit a simple pole if $k_\perp$ equals the magnitude Q_h of a vector from the translated lattice. At the same time, the problem presents no symmetry, all the vectors $\mathbf{Q}_h$ are different and, consequently, all the poles of the lattice sums are nondegenerate. The behavior close to a pole is given by the formula

$$S_\ell^Y(k_\perp) \sim \frac{4}{{k_\perp}^2-Q_h^2}\,i^\ell\,e^{i\ell\theta_h}\ , \tag{56}$$

the residue of the corresponding pole being a complex quantity. This formula also applies to S_0^Y. In addition, all the lattice sums exhibit a simple pole at $k_\perp = k_\perp^i$, for $\mathbf{K}_h = 0$.

There is an interesting special case when the incident wave vector is confined in the xz plane ($\theta = 0$):

$$\mathbf{k}^i = -\frac{2\pi}{\lambda}(\sin\varphi, 0, \cos\varphi) = (k_\perp^i, 0, k_\parallel^i)\ ,$$

and the definition of the lattice sums takes the form

$$\mathcal{S}_\ell(k_\perp) = {\sum_{n,m}}' H_\ell^{(1)}(k_\perp\sqrt{n^2+m^2})\,e^{i\ell\arctan(m/n)}\,e^{ink_\perp^i},$$

where the prime indicates that the term with $n = m = 0$ is to be omitted. For this particular off-axis incidence the lattice sums satisfy the relation

$$\mathcal{S}_{-\ell}(k_\perp) = (-1)^\ell\mathcal{S}_\ell(k_\perp)\ ,$$

and, therefore,

$$\mathcal{S}_{-\ell}^Y(k_\perp) = (-1)^\ell\mathcal{S}_\ell^Y(k_\perp)\ .$$

Actually, in this case, the symmetry with respect to the reflection $y \to -y$ is preserved. Consequently, from (50), we deduce that the lattice sums $\mathcal{S}_\ell^Y$ are real for even ℓ and imaginary for odd ℓ.

The lattice defined by the set $\{\mathbf{Q}_h\}$ is obtained from the reciprocal lattice $\{\mathbf{K}_h\}$ by a translation along the x

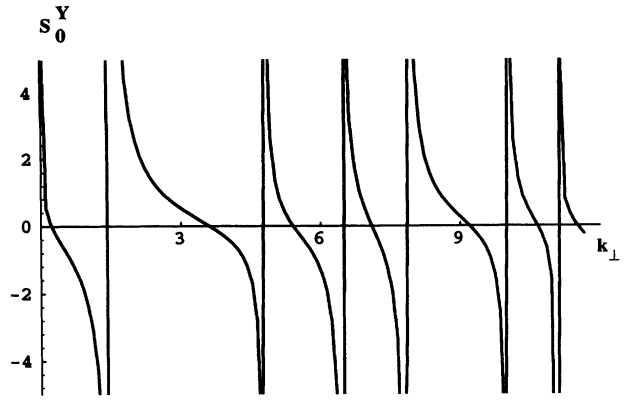

FIG. 4. Off-axis incidence. $\mathcal{S}_0^Y(k_\perp)$ for $\lambda = 2.3$, $\varphi = \pi/12$ and $\theta = 0$.

axis, introduced by $k_\perp^i$. We have similar relations to (54) and (55) for the behavior of the lattice sums for small $k_\perp$. The lattice sums also preserve the simple pole at $k_\perp = k_\perp^i$, corresponding to the translation of the origin. All the other poles are degenerate in two ways. To make clear this behavior we separate the reciprocal lattice, excepting the origin, into two kinds of patterns, each of them containing four points. These patterns are defined by the sets $\{2\pi(\pm n, 0), 2\pi(0, \pm n)\}$, containing two equidistant points on each axis, and $\{2\pi(\pm n, \pm m)\}$, with no point on the axes, i.e., we have patterns containing four vectors $\mathbf{K}_h$ of the same magnitude but different directions. Each pattern, of the first or second kind, contributes to only one pole in (29). The translation by $k_\perp^i$, along the x axis, breaks the symmetry and changes the patterns of the first kind such that they will contain three different vector magnitudes, while the patterns of the second kind will contain only two different vector magnitudes. This explains the splitting of poles, from the case of normal incidence, into three or two distinct poles for $\theta = 0$.

A similar situation appears if $\mathbf{k}_\perp^i$ is confined in the yz plane ($\theta = \pm\pi/2$), or, more generally, if θ equals an integer number of $\pi/4$.

In Figs. 4 and 5 we give two examples for the behavior

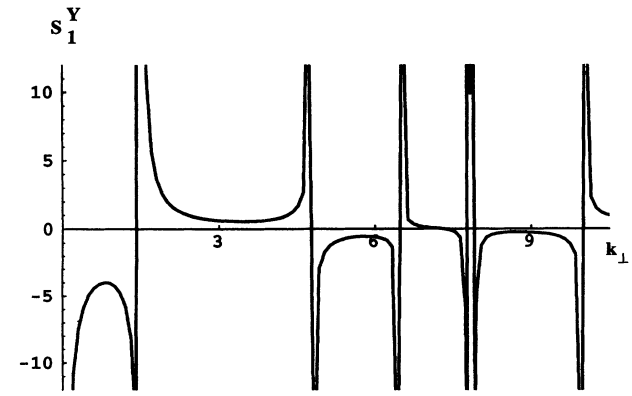

FIG. 5. Off-axis incidence. $\mathrm{Im}[\mathcal{S}_1^Y(k_\perp)]$ for $\lambda = 2.3$, $\varphi = \pi/12$, and $\theta = 0$.

of $\mathcal{S}_0^Y$ and $\mathcal{S}_1^Y$ as functions of $k_\perp$, when $\theta = 0$. Note that $\mathcal{S}_0^Y$ is real, while $\mathcal{S}_1^Y$ is pure imaginary. Therefore, the figures display the real part of $\mathcal{S}_0^Y$ and the imaginary part of $\mathcal{S}_1^Y$, respectively.

IV. NEUMANN SERIES FOR THE GREEN'S FUNCTION

In the case of normal incidence, by means of (15) we obtain the expansion of the doubly periodic Green's function (9), defined over the direct lattice, as a Neumann series, the coefficients being the lattice sums:

$$G_d(\mathbf{r};\boldsymbol{\rho}) = \frac{i\pi}{2} H_0^{(1)}(k_\perp \mid \mathbf{r} - \boldsymbol{\rho} \mid) + \frac{i\pi}{2} \sum_{\ell=-\infty}^{\infty} S_{4\ell}(k_\perp) J_{4\ell}(k_\perp \mid \mathbf{r} - \boldsymbol{\rho} \mid) e^{-i4\ell\beta}. \tag{57}$$

Therefore, the doubly periodic Green's function (9) contains all the symmetry properties of the lattice.

Let us assume that $\rho = 0$. Then, we replace the lattice sums by their expression $S_{4\ell}(k_\perp) = -\delta_{\ell,0} + iS_{4\ell}^Y(k_\perp)$, so that the Green's function becomes

$$G_d(\mathbf{r}) = -\frac{\pi}{2} Y_0(k_\perp r) - \frac{\pi}{2} \sum_{\ell=-\infty}^{\infty} S_{4\ell}^Y(k_\perp) J_{4\ell}(k_\perp r)\, e^{-i4\ell\theta}\,. \tag{58}$$

Here, $r = \sqrt{x^2 + y^2}$ and $\theta = \arctan(y/x)$, with r restricted to the central unit cell.

Taking into account that, for large ℓ, we may approximate p.p. $S_{4\ell}^Y \sim 4Y_{4\ell}(k_\perp d)$, we apply the Kummer method [12] to accelerate the convergence of the series in (58):

$$G_d(\mathbf{r}) = -\frac{\pi}{2} Y_0(k_\perp r) - \frac{\pi}{2} S - \frac{\pi}{2} \sum_{\ell=-\infty}^{\infty} [S_{4\ell}^Y(k_\perp) - 4Y_{4\ell}(k_\perp d)] \times J_{4\ell}(k_\perp r) e^{-i4\ell\theta}\,, \tag{59}$$

where

$$S = 4 \sum_{\ell=-\infty}^{\infty} Y_{4\ell}(k_\perp d) J_{4\ell}(k_\perp r)\, e^{-i4\ell\theta} = Y_0(k_\perp \mid \mathbf{r} - d\mathbf{i} \mid) + Y_0(k_\perp \mid \mathbf{r} + d\mathbf{i} \mid) + Y_0(k_\perp \mid \mathbf{r} - d\mathbf{j} \mid) + Y_0(k_\perp \mid \mathbf{r} + d\mathbf{j} \mid)\,,$$

$\mathbf{i}$ and $\mathbf{j}$ being the unit vectors along the x and y axes, respectively.

This result is valid only within the central unit cell, where $r \le d/\sqrt{2} < d$.

From the definition (7) we deduce

$$S_{-\ell}(k_\perp) = (-1)^\ell S_\ell(k_\perp)$$

and, from (59), by replacing $d = 1$, we obtain

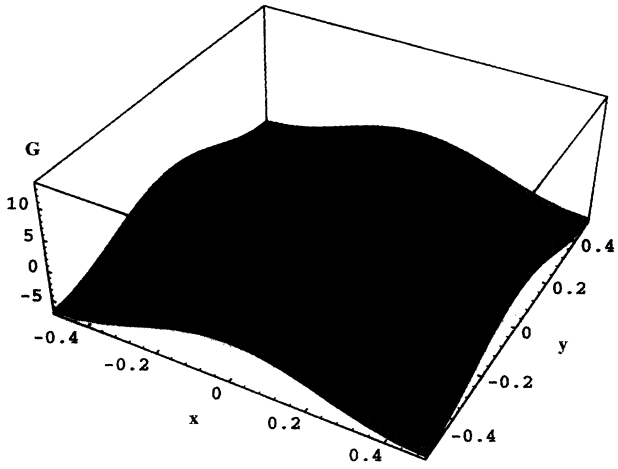

FIG. 6. Normal incidence. $G(x,y)$ for $k_\perp = 6$.

$$G_d(\mathbf{r}) = -\frac{\pi}{2}\Big\{Y_0(k_\perp r) + S + \Big[S_0^Y(k_\perp) - 4Y_0(k_\perp)\Big]J_0(k_\perp r)\Big\} - \pi\sum_{\ell=1}^{\infty}\Big[S_{4\ell}^Y(k_\perp) - 4Y_{4\ell}(k_\perp)\Big] \times J_{4\ell}(k_\perp r)\cos(4\ell\theta). \tag{60}$$

We also have to mention that this formula is true only for a square lattice and within the central unit cell, in the case of normal incidence. From the comments made in relation to Table II, we see that the series in the representation (60) should be rapidly convergent.

In Fig. 6 we display the surface plot obtained from (60), for $k_\perp = 6$.

For off-axis incidence, and $\rho = 0$, the Green's function (38) takes the form

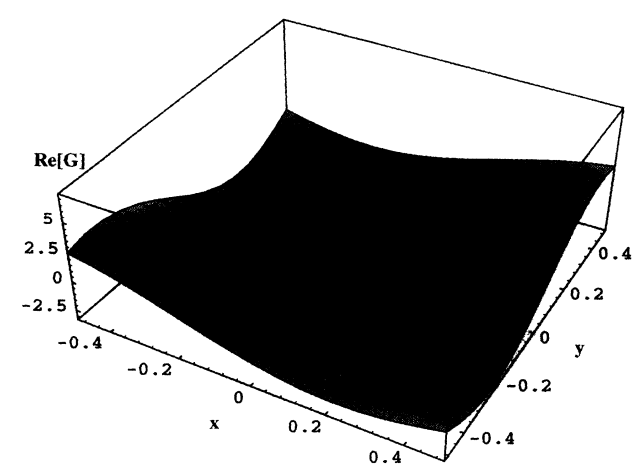

FIG. 7. Off-axis incidence. $\mathrm{Re}[G(x,y)]$ for $\lambda = 2.3$, $\theta = 5\pi/6$, $\varphi = \pi/2$, and $k_\perp = 6$.

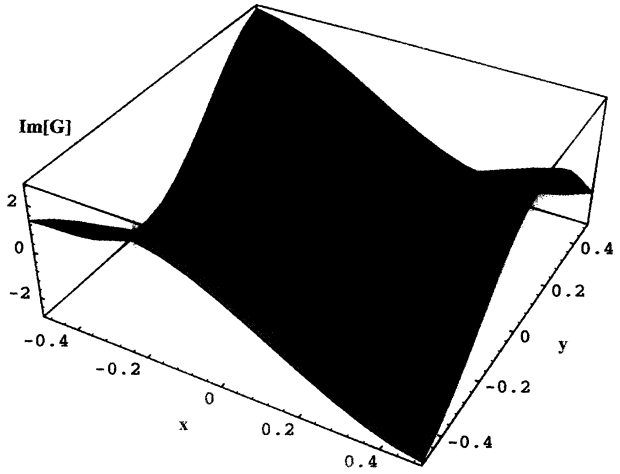

FIG. 8. Off-axis incidence. $\mathrm{Im}[G(x,y)]$ for $\lambda = 2.3$, $\theta = 5\pi/6$, $\varphi = \pi/2$, and $k_\perp = 6$.

$$G_d(\mathbf{r}) = \frac{i\pi}{2}H_0^{(1)}(k_\perp r) + \frac{i\pi}{2}\sum_{\ell=-\infty}^{\infty}\mathcal{S}_\ell(k_\perp)J_\ell(k_\perp r)e^{-i\ell\theta} = -\frac{\pi}{2}Y_0(k_\perp r) - \frac{\pi}{2}\sum_{\ell=-\infty}^{\infty}\mathcal{S}_\ell^Y(k_\perp)J_\ell(k_\perp r)e^{-i\ell\theta}. \tag{61}$$

Here, the lattice sums $\mathcal{S}_\ell^Y$ are complex for all values of ℓ and $\mathcal{S}_{-\ell}^Y(k_\perp) = \mathcal{S}_\ell^{Y*}(k_\perp)$. Kummer's method could once again be applied to (61), to exhibit explicitly the nearest-neighbor terms.

In Figs. 7 and 8 we display the surface plot of the real and imaginary parts of $G_d(\mathbf{r})$, for the incidence angles $\varphi = \pi/2$, $\theta = 5\pi/6$, the wavelength of the incident radiation being $\lambda = 2.3$ and $k_\perp = 6$. In the surface plots of G_d, note that the central peak in fact represents an under-sampled logarithmic singularity.

As a check of these results, Fig. 9 displays the sur-

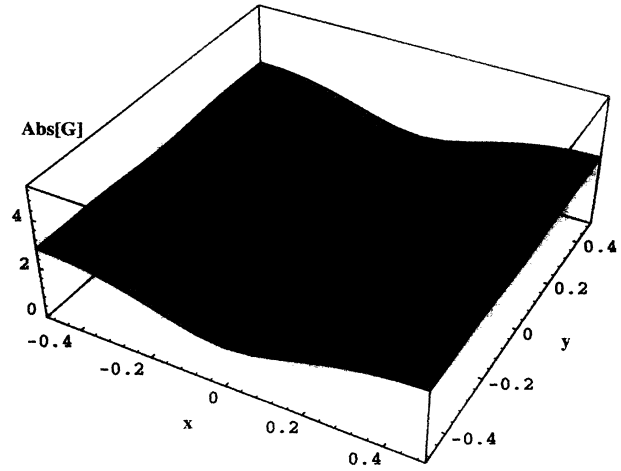

FIG. 9. Off-axis incidence. $\mathrm{Abs}[G(x,y)]$ for $\lambda = 2.3$, $\theta = 5\pi/6$, $\varphi = \pi/2$, and $k_\perp = 6$.

TABLE III. Numerical values of the Green's function along the boundaries of the unit cell in Fig. 9. We truncated the series in (61) at $\ell = 20$ and used $m = 1$ in (52). The first column displays the values of x and y, respectively.

	$(x,-1/2)$	$(x,+1/2)$	$(-1/2,y)$	$(+1/2,y)$
$-1/2$	2.831 05	2.831 10	2.831 05	2.831 10
	2.790 23	2.790 26	2.842 40	2.842 40
	2.667 21	2.667 23	2.864 88	2.864 84
	2.463 44	2.463 47	2.873 30	2.873 23
	2.191 49	2.191 51	2.84 902	2.848 92
	1.888 26	1.888 28	2.795 58	2.795 48
	1.629 45	1.629 46	2.739 87	2.739 80
0	1.522 93	1.522 93	2.716 01	2.716 01
	1.629 46	1.629 45	2.739 80	2.739 87
	1.888 28	1.888 26	2.795 48	2.795 58
	2.191 51	2.191 49	2.848 92	2.849 02
	2.463 47	2.463 44	2.873 23	2.873 30
	2.667 23	2.667 21	2.864 84	2.864 88
	2.790 26	2.790 23	2.842 40	2.842 40
$+1/2$	2.831 10	2.831 05	2.831 10	2.831 05

face plot of $|G_d(\mathbf{r})|$, which, according to (37), is a doubly periodic function over the direct lattice.

In Tables III and IV we illustrate a numerical test of the quasiperiodicity condition (37) by means of the numerical values of the Green's function, given by (61), along the boundaries of the unit cell. The lattice sums in Tables III and IV have been evaluated by summing over the same region of reciprocal space. However, in Table III we have used Eq. (52) with $m = 1$, and in Table IV with $m = 6$. The lattice sums in the second case are much more accurate, as can be seen from the quasiperiodicity test.

TABLE IV. Numerical values of the Green's function along the boundaries of the unit cell in Fig. 9. We truncated the series in (61) at $\ell = 20$ and used $m = 6$ in (52). The first column displays the values of x and y, respectively.

	$(x,-1/2)$	$(x,+1/2)$	$(-1/2,y)$	$(+1/2,y)$
$-1/2$	2.831 06	2.831 09	2.831 06	2.831 09
	2.790 24	2.790 25	2.842 39	2.842 40
	2.667 24	2.66 723	2.864 85	2.864 85
	2.463 47	2.463 47	2.873 25	2.873 25
	2.191 51	2.191 51	2.848 96	2.848 96
	1.888 28	1.888 28	2.795 53	2.795 53
	1.629 45	1.629 45	2.739 84	2.739 84
0	1.522 92	1.522 92	2.716 03	2.716 03
	1.629 45	1.629 45	2.739 84	2.739 84
	1.888 28	1.888 28	2.795 53	2.795 53
	2.191 51	2.191 51	2.848 96	2.848 96
	2.463 47	2.463 47	2.873 25	2.873 25
	2.667 23	2.667 24	2.864 85	2.864 85
	2.790 25	2.790 24	2.842 40	2.842 39
$+1/2$	2.831 09	2.831 06	2.831 09	2.831 06

V. LATTICE SUMS AND THE GREEN'S FUNCTION FOR IMAGINARY WAVE NUMBER

In the case of an imaginary $k_\perp$, we replace $k_\perp$ by $i\,k_\perp$, and the Green's function is the elementary solution of the inhomogeneous Helmholtz equation

$$\Delta_2 G(\mathbf{r}) - k_\perp^2 G(\mathbf{r}) = -2\pi\delta(\mathbf{r}) \ . \tag{62}$$

Then, from (5), we obtain the formula

$$G(\mathbf{r}) = K_0(k_\perp r) \ , \tag{63}$$

where K is the modified Bessel function. Consequently, we have the quasiperiodic Green's function:

$$G_d(\mathbf{r};\boldsymbol{\rho}) = \sum_p K_0(k_\perp \mid \mathbf{r} - \mathbf{R}_p - \boldsymbol{\rho} \mid) \, e^{i\mathbf{k}_\perp^i \cdot \mathbf{R}_p} \ , \tag{64}$$

in the direct lattice space, and

$$G_r(\mathbf{r};\boldsymbol{\rho}) = \frac{1}{2\pi} \sum_h \frac{e^{i\mathbf{Q}_h\cdot(\mathbf{r}-\boldsymbol{\rho})}}{Q_h^2 + k_\perp^2} \ , \tag{65}$$

in the reciprocal lattice space.

We may apply the same method as in Sec. III B, or, simply replacing in (41) and (48) the Bessel and Hankel functions, whose argument depends on $k_\perp$, by the corresponding modified Bessel functions [12]:

$$J_n(ik_\perp\xi) = i^n \, I_n(k_\perp\xi) \ ,$$
$$H_n^{(1)}(ik_\perp\xi) = (-i)^{n+1} \, \frac{2}{\pi} \, K_n(k_\perp\xi) \ .$$

From (41) we obtain

$$\begin{aligned} \mathcal{S}_\ell(ik_\perp) &= \sum_{p\neq 0} H_\ell^{(1)}(ik_\perp R_p) \, e^{i\ell\varphi_p} \, e^{i\mathbf{k}_\perp^i\cdot\mathbf{R}_p} \\ &= (-i)^{\ell+1} \, \frac{2}{\pi} \sum_{p\neq 0} K_\ell(k_\perp R_p) \, e^{i\ell\varphi_p} \, e^{i\mathbf{k}_\perp^i\cdot\mathbf{R}_p} \\ &\equiv (-i)^{\ell+1} \, \frac{2}{\pi} \, \widetilde{S}_\ell(k_\perp) \ . \end{aligned} \tag{66}$$

Further, substituting in (48), multiplying by $\xi^{\ell+1}$ and integrating over ξ from 0 to 1, the system (48) becomes

$$\begin{aligned} \widetilde{S}_\ell(k_\perp) I_{\ell+1}(k_\perp) = &\left[K_1(k_\perp) - \frac{1}{k_\perp}\right] \delta_{\ell,0} \\ &+ 2\pi k_\perp i^\ell \sum_h \frac{J_{\ell+1}(Q_h)}{Q_h(Q_h^2 + k_\perp{}^2)} \, e^{i\ell\theta_h} . \end{aligned} \tag{67}$$

For normal incidence, we have to separate from the series the term for $h = 0$ so that the system (67) takes the form

$$\begin{aligned} \widetilde{S}_\ell(k_\perp) I_{\ell+1}(k_\perp) = &\left[K_1(k_\perp) + \frac{\pi - 1}{k_\perp}\right] \delta_{\ell,0} \\ &+ 2\pi k_\perp i^\ell \sum_{h\neq 0} \frac{J_{\ell+1}(K_h)}{K_h(K_h^2 + k_\perp{}^2)} \, e^{i\ell\theta_h} . \end{aligned} \tag{68}$$

The method to accelerate the series, described in Sec. III B, may be also applied to (67) and (68).

We mention that in all cases $\widetilde{S}_0$ is real and exhibits an essential singularity at the origin, generated by the logarithmic behavior of K_1 for small arguments [12]. All the other lattice sums have a pole of order ℓ at the origin. In contrast with the case of real $k_\perp$, there are no other poles along the imaginary axis in the plane of complex $k_\perp$. The lattice sums are monotonic functions of $k_\perp$, tending to zero for large $k_\perp$.

By applying the addition theorem for the K functions [14], we may express the Green's function (64) as a Neumann series in terms of the I_ℓ functions:

$$G_d(\mathbf{r}) = K_0(k_\perp r) + \sum_{\ell=-\infty}^{\infty} \widetilde{S}_\ell(k_\perp)\, I_\ell(k_\perp r)\, e^{-i\ell\theta} \ .$$

For a TM mode, the system corresponding to (40), obtained from the Rayleigh method, has the form

$$\frac{K_n(k_\perp a)}{I_n(k_\perp a)}(-i)^n B_{-n} + \sum_{k=-\infty}^{\infty} (-i)^k B_k \widetilde{S}_{k+n}(k_\perp) = 0. \quad (69)$$

VI. CONCLUSIONS

We have discussed methods for representing in absolutely convergent form the lattice sums arising in doubly periodic electromagnetic diffraction problems. The final expressions for the lattice sums are quite simple, but remarkable in that they contain an arbitrary integer, which permits an arbitrary degree of acceleration of the convergence of the series. We have shown how these lattice sums may be used to construct expressions for the Green's function which converge well throughout the unit cell. The results presented here will, therefore, be of great use to those interested in electromagnetic diffraction by doubly periodic systems. Note that, although we have introduced the lattice sums and Green's function in the context of the diffraction by an array of perfectly conducting cylinders, both, in fact do not depend on cylinder conductivity. Consequently, they can be used in diffraction problems involving square arrays of dielectric or lossy metallic cylinders.

ACKNOWLEDGMENTS

The authors wish to acknowledge a valuable suggestion by Professor D. Melrose, regarding the acceleration of lattice sums series. This work was undertaken while one of the authors (N.A. Nicorovici) was the recipient of an Australian Research Council Grant. The support of the Science Foundation for Physics within the University of Sydney is also acknowledged.

APPENDIX

We denote by $\boldsymbol{\xi} = \mathbf{r} - \boldsymbol{\rho}$, $\beta = \arg(\mathbf{r} - \boldsymbol{\rho})$, and assume that $|\mathbf{r}| < |\boldsymbol{\rho}|$.

From Fig. 2 we have $\beta = \alpha + \theta$, and we apply Graf's addition theorem [12,14], which, in our case, takes the form

$$J_\ell(k_\perp \xi)e^{i\ell\alpha} = \sum_{k=-\infty}^{\infty} J_{\ell+k}(k_\perp \rho)J_k(k_\perp r)e^{ik\theta}e^{-ik\psi}. \quad \text{(A1)}$$

We use the complex conjugate of this expression in the right hand side of (15) so that

$$\begin{aligned} J_\ell(k_\perp \xi)e^{-i\ell\beta} &= J_\ell(k_\perp \xi)e^{-i\ell\alpha}e^{-i\ell\theta} \\ &= e^{-i\ell\theta} \sum_{k=-\infty}^{\infty} J_{\ell+k}(k_\perp \rho)J_k(k_\perp r)e^{-ik\theta}e^{ik\psi} \\ &= \sum_{k=-\infty}^{\infty} J_{\ell+k}(k_\perp \rho)J_k(k_\perp r)e^{-i(k+\ell)\theta}e^{ik\psi} \ , \end{aligned} \quad \text{(A2)}$$

and, changing k into $-k$, we obtain (16).

We apply the same method to obtain (17).

[1] Lord Rayleigh, Philos. Mag. **34**, 481 (1892).
[2] P.P. Ewald, Ann. Phys. (Leipzig) **64**, 253 (1921).
[3] R.C. McPhedran and D.H. Dawes, J. Electromagn. Waves Appl. **6**, 1327 (1992).
[4] Van der Hoff and G.C. Benson, Can. J. Phys. **31**, 1087 (1953).
[5] G.C. Benson and H.P. Schreiber, Can. J. Phys. **33**, 529 (1955).
[6] C.A. Scholl, Proc. Phys. Soc. London **92**, 434 (1967).
[7] M.L. Glasser, J. Math. Phys. **14**, 409 (1973); **14**, 701 (1973); **15**, 188 (1974); **16**, 1237 (1974).
[8] A.P. Smith and N.W. Ashcroft, Phys. Rev. B **38**, 12 942 (1988).
[9] P.M. Morse and H. Feshbach, *Methods of Theoretical Physics* (McGraw-Hill, New York, 1953), Vol. 1, Chap. 7.
[10] L. Jansen and M. Boon, *Theory of Finite Groups* (North Holland, Amsterdam, 1967).
[11] J.C. Slater, *Solid-State and Molecular Theory* (Wiley, New York, 1975).
[12] M. Abramowitz and I.A. Stegun, *Handbook of Mathematical Functions with Formulas, Graphs and Mathematical Tables* (Dover, New York, 1972).
[13] R. Courant and D. Hilbert, *Methods of Mathematical Physics* (Interscience, New York, 1953).
[14] N.N. Lebedev, *Special Functions and Their Applications* (Prentice-Hall, Englewood Cliffs, NJ, 1965).

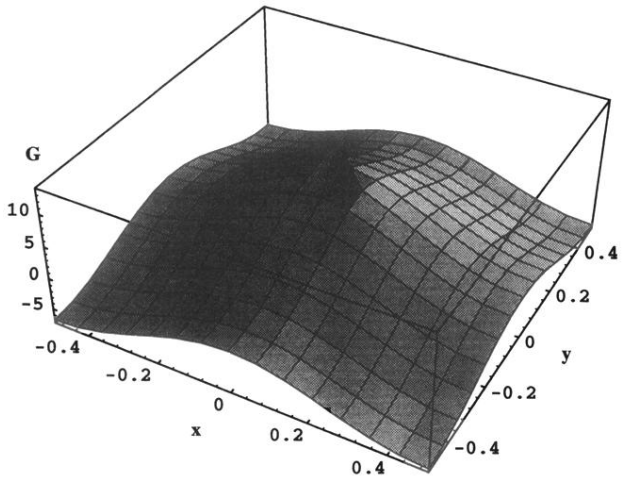

FIG. 6. Normal incidence. $G(x, y)$ for $k_\perp = 6$.

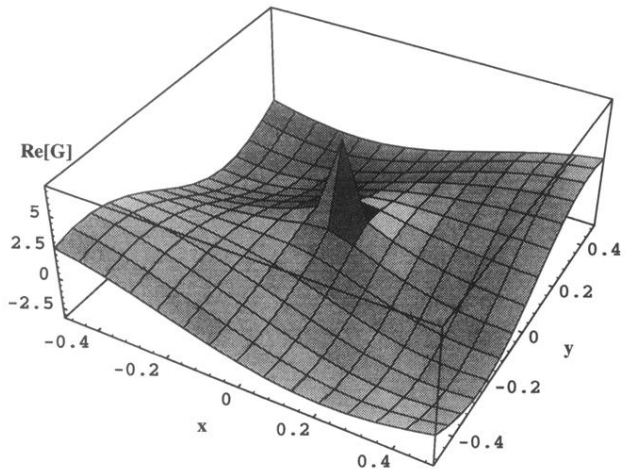

FIG. 7. Off-axis incidence. $\mathrm{Re}[G(x,y)]$ for $\lambda = 2.3$, $\theta = 5\pi/6$, $\varphi = \pi/2$, and $k_\perp = 6$.

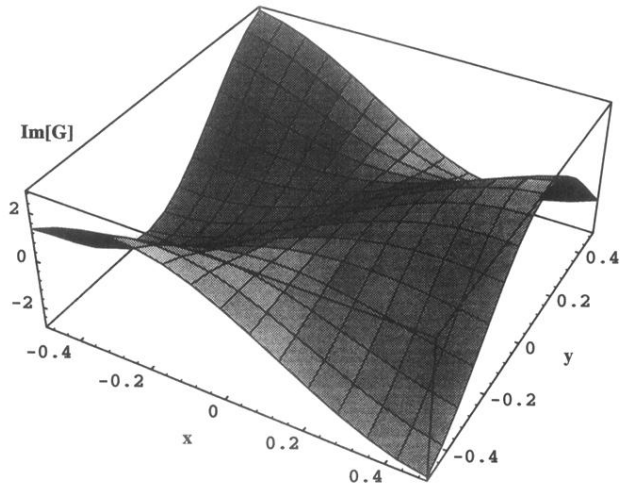

FIG. 8. Off-axis incidence. $\mathrm{Im}[G(x,y)]$ for $\lambda = 2.3$, $\theta = 5\pi/6$, $\varphi = \pi/2$, and $k_\perp = 6$.

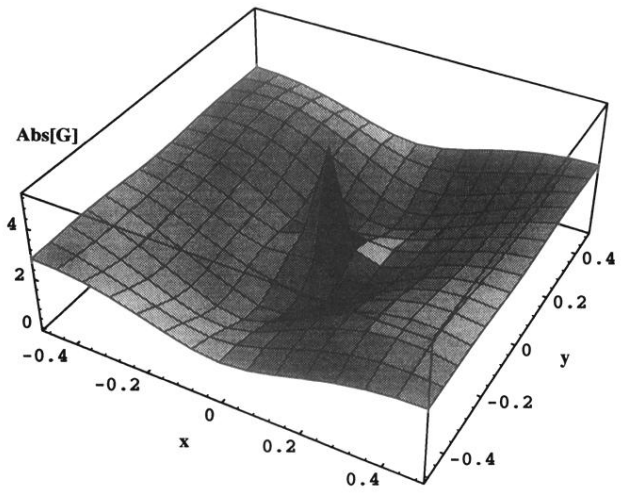

FIG. 9. Off-axis incidence. Abs$[G(x,y)]$ for $\lambda = 2.3$, $\theta = 5\pi/6$, $\varphi = \pi/2$, and $k_\perp = 6$.